Virology 283, 1–6 (2001)
doi:10.1006/viro.2001.0860, available online at http://www.idealibrary.com on IDEAL®

RAPID COMMUNICATION

Vesicular Release of Ebola Virus Matrix Protein VP40

Joanna Timmins, Sandra Scianimanico, Guy Schoehn, and Winfried Weissenhorn[1]

EMBL, 6 rue Jules Horowitz, B.P. 181, 38042 Grenoble, France

Received September 20, 2000; returned to author for revision October 26, 2000, accepted February 7, 2001

We have analysed the expression and cellular localisation of the matrix protein VP40 from Ebola virus. Full-length VP40 and an N-terminal truncated construct missing the first 31 residues [VP40(31–326)] both locate to the plasma membrane of 293T cells when expressed transiently, while a C-terminal truncation of residues 213 to 326 [VP40(31–212)] shows only expression in the cytoplasm, when analysed by indirect immunofluorescence and plasma membrane preparations. In addition, we find that full-length VP40 [VP40(1–326)] and VP40(31–326) are both released into the cell culture supernatant and float up in sucrose gradients. The efficiency of their release, however, is dependent on the presence of the N-terminal 31 residues. VP40 that is released into the supernatant is resistant to trypsin digestion, a finding that is consistent with the formation of viruslike particles detected by electron microscopy. Together, these results provide strong evidence that Ebola virus VP40 is sufficient for virus assembly and budding from the plasma membrane.

INTRODUCTION

Ebola virus and Marburg virus (Filoviridae) are nonsegmented negative-strand RNA viruses (Mononegavirales) that cause severe hemorrhagic fever in humans (*1–3*). The matrix protein VP40 is a major structural protein from Ebola virus and is thought to play a key role in virus assembly and release, which takes place at the plasma membrane (*4*, *5*). Viral matrix proteins are multifunctional proteins that interact with cellular membranes and viral components such as the cytoplasmic tails of glycoproteins as well as the ribonucleoprotein particle (RNP) (*6*) in a process which triggers the formation and the release of infectious particles from infected cells. The Ebola virus matrix protein binds preferentially to liposomes containing high amounts of negatively charged phospholipids *in vitro* (*7*). A similar *in vitro* membrane association behaviour has been observed for matrix proteins from vesicular stomatitis virus (VSV) (*8*) and influenza virus (*9*) as well as retroviral matrix proteins (*10*). Ebola virus VP40 is a monomer in solution, consisting of two domains (*11*). The C-terminal domain is absolutely required for membrane association *in vitro* and the removal of most of the C-terminal domain by trypsin digestion has been shown to induce hexamerisation of VP40 (*7*). The same hexamerisation pattern is observed when destabilizing the interdomain region by mutagenesis or by urea treatment *in vitro* as well as by binding of VP40 to liposomes (*12*). Although it has been shown that the VSV matrix protein is released from cells in the form of lipid vesicles (*13, 14*), the efficiency of assembly and particle release depends on interactions with cellular proteins mediated by a conserved WW domain binding motif (PPXY; PY motif) (*15*). A similar PY motif is found at the N-terminus of Ebola virus VP40 where it mediates the interaction with a ubiquitin ligase in a process which was proposed to be important in budding (*16*). In contrast, most viral matrix proteins do not trigger the release of vesicles from cells and virus-particle formation involves multiple interactions (*17–20*). Here we demonstrate that the matrix protein VP40 from Ebola virus associates with the plasma membrane *in vivo*. This is dependent on the presence of the C-terminal domain but is not affected by the removal of the N-terminal PY motif. Both findings are in agreement with data obtained *in vitro* on VP40 membrane association (*7*). In addition, we show that VP40 is released into the cell culture supernatant when expressed by itself and is found associated with lipid vesicles, which resemble filovirus-like particles as determined by electron microscopy. However, the efficiency of particle release is approximately fivefold decreased upon deletion of the proposed WW-domain binding motif, consistent with recently published findings (*16*). This suggests that, on its own, VP40 is able to bud through the plasma membrane and thus contains important properties for the assembly and the release of Ebola virus particles.

Results. Ebola virus VP40 consists of two domains that form a closed conformation in solution (Fig. 1) (*11*). The

[1] To whom correspondence and reprint requests should be addressed. E-mail: weissen@embl-grenoble.fr.

0042-6822/01 $35.00

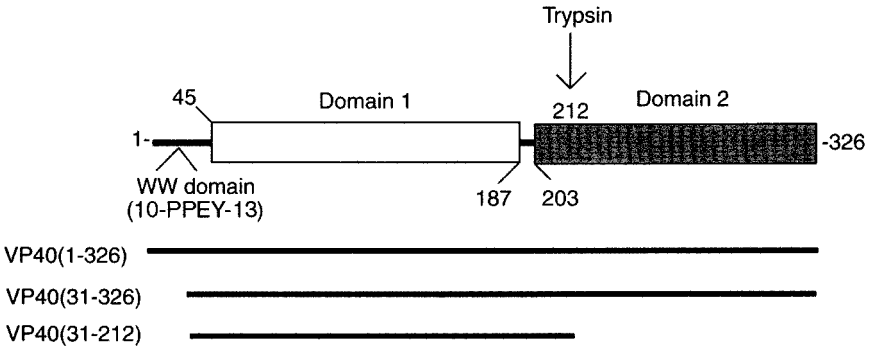

FIG. 1. VP40 contains two structurally related domains that are indicated schematically. The two domains are shown as boxes based on the crystal structure of VP40 (*11*). The N-terminal domain contains a potential WW domain-binding motif as indicated which is not present in the crystal structure. VP40 constructs used for expression are shown.

N-terminal part, which is not present in the crystal structure, contains a PY motif (*15*). We transfected 293T cells with cDNAs corresponding to VP40(1–326), VP40(31–326), and VP40(31–212) (Fig. 1) to determine their cellular localisation. Both VP40(1–326) and VP40(31–326) are expressed throughout the cytoplasm but concentrate in patches along the plasma membrane as seen by indirect immunofluorescence (Figs. 2A and 2B). In contrast, the C-terminally truncated construct VP40(31–212) does not localise to the plasma membrane and shows only diffuse distribution throughout the cytoplasm (Fig. 2C). No staining can be seen with nontransfected or mock-transfected cells (data not shown). These results were confirmed by the analysis of plasma membrane preparations derived from transfected 293T cells expressing VP40(1–326), VP40(31–326), and VP40(31–212). Full-length VP40 migrates at approximately 36 kDa, the N-terminal truncated form slightly faster and C-terminally truncated VP40 migrates at approximately 25 kDa when analysed by SDS–PAGE and Western blotting (Fig. 3). Both constructs, VP40(1–326) and VP40(31–326), associate with the plasma membrane (Fig. 3A). Comparison of the total protein expressed (Fig. 3A, lanes 1 and 3) and the amount found to interact with the plasma membrane, shows approximately 7% membrane association for both constructs (Fig. 3B, lanes 2 and 4). This indicates that the first 31 residues of VP40 are dispensable for its cellular localisation and does not affect the efficiency of membrane association, similar to the results obtained *in vitro* (*7*). Deletion of most of the C-terminal domain of VP40 resulted in solely cytoplasmic expression of VP40(31–212) and no protein was detected to be associated with the plasma membrane (Fig. 3A, lanes 5 and 6), which confirms the role of the C-terminal domain in membrane targeting *in vivo*. This is also consistent with the immunofluorescence staining (Fig. 2C) and liposome binding assays performed *in vitro* (*7*).

Western blot analysis of the expression pattern of all three constructs analysed indicates that full-length VP40(1–326) as well as VP40(31–326) are both released into the cell culture medium (Fig. 3B, lanes 1s and 3s).

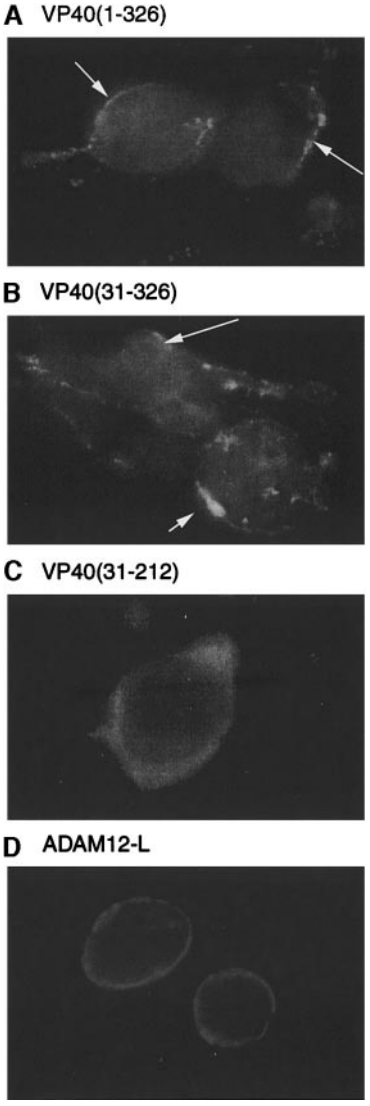

FIG. 2. Intracellular distribution of VP40 constructs and ADAM12-L determined by indirect immunofluorescence. 293T cells, transfected with pVP40(1–326) (A), with pVP40(31–326) (B), with pVP40(31–212) (C), as well as with pADAM12-L (D), were fixed in methanol/acetone 72 h posttransfection. VP40 was detected with a rabbit polyclonal antiserum and ADAM12-L with a myc-tag specific mAb and fluorescein-conjugated secondary antibodies. Cells were observed under a 100× oil immersion objective with a Zeiss Axioscope microscope.

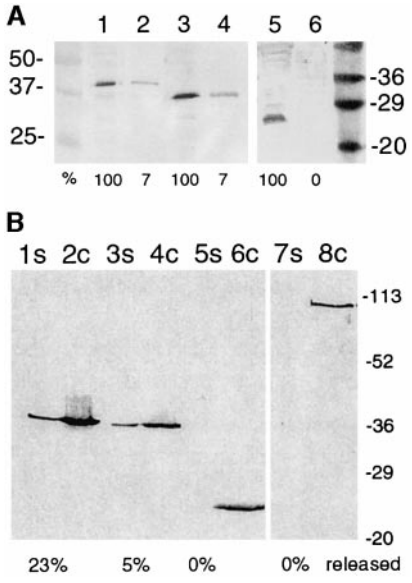

FIG. 3. (A) Plasma membrane preparations of VP40 expressed in 293T cells. Lanes 1 and 3 correspond to the total amount of VP40(1–326) and VP40(31–326) expressed from 2×10^5 293T cells (100%). Lanes 2 and 4 correspond to the amount of VP40(1–326) and VP40(31–326) found to be associated with the plasma membrane compared to the total amount (7% in each case). In contrast, VP40(31–212) does not associate with the plasma membrane; lane 5, VP40(31–212) expressed from 4×10^5 cells (100%) compared to lane 6, plasma membrane fraction corresponding to 4×10^5 cells (0%). (B) Western blot analysis of VP40 expression in 293T cells. Cells were lysed 72 h posttransfection and cell extracts (c) and cell culture supernatants (s) were separated on 12% SDS–PAGE; lanes 1s and 2c, VP40(1–326); lanes 3s and 4c, VP40(31–326); lanes 5s and 6c, VP40(31–212); and lanes 7s and 8c, ADAM12L. VP40-specific bands were visualised using a VP40-specific polyclonal antiserum and the anti-myc antibody was used to detect ADAM12-L by Western blot analysis. Quantification of released VP40 indicates that 5% of VP40(31–326) and 23% of VP40(1–326) are released into the culture medium when compared to total cell lysates (100%). Molecular weight markers are indicated in kilodaltons.

Twenty-three percent of full-length VP40 is detected in the cell culture supernatant when compared to the total amount of protein expressed; however, only 5% of total VP40(31–326) is released (Fig. 3B; lanes 3s and 4c). The release of VP40(31–326) indicates a specific role for the N-terminus containing the PY motif. The loss of membrane targeting activity of VP40(31–212) is also consistent with no release of VP40(31–212) missing most of the C-terminal domain (Fig. 3B, lanes 5s and 6c). To further substantiate that the presence of VP40 in the supernatant is not due to the release of protein by cell lysis, 293T cells were also transfected with a full-length clone of ADAM12-L, a type I membrane protein (*21*). Transfections of all four constructs were done in parallel, and no significant cell death was observed at the time of harvesting the cells and the supernatants. ADAM12-L is clearly expressed at the cell surface of 293T cells as expected (Fig. 2D) and an expression band corresponding to the correct molecular weight can be seen in a whole-cell extract but not in the cell culture supernatant (Fig. 3B, lanes 7 and 8). These data suggest that specific membrane association of VP40(1–326) and VP40(31–326) is necessary for the release of VP40 into the medium. This interaction does not occur with VP40 expressed only in the cytoplasm [such as VP40(31–212)] nor with a plasma membrane anchored protein such as ADAM12-L, as expected.

The supernatants of cells transfected with VP40 constructs were further analyzed by sucrose gradient centrifugation. These results show that VP40(1–326) (Fig. 4A) as well as VP40(31–326) (Fig. 4B) migrate toward the top in a discontinuous sucrose gradient and most of the protein is found in fractions 4 to 6 or 3 to 5 (Figs. 4A and 4B). Some protein remains in the bottom fractions 8 and 9 (Figs. 4A and 4B). Therefore, both VP40 proteins probably float with vesicles in upper fractions containing 20–30% sucrose. Trypsin digestion of vesicle-bound VP40(1–326) also indicates that it is protected from proteolysis. Incubation of VP40(1–326) derived from fraction 4 of the sucrose gradient (Fig. 4A) with trypsin showed no proteolysis (Fig. 4C; lane 2). However, solubilisation of VP40 from the same sucrose gradient fraction with Triton X-100 shows that detergent treatment renders VP40 sensitive to trypsin, resulting in smaller proteolytic products (Fig. 4C, lane 3). Electron microscopy of vesicles released into the cell culture supernatant containing VP40(1–326) and purified by sucrose gradient centrifugation reveals the presence of filamentous viruslike particles. A typical particle shows a diameter of approximately 80 nm and a length of 1000 nm (Fig. 4D). This suggests further that VP40 assembles at the plasma membrane in a process which is capable of pinching off vesicles that resemble viruslike structures.

Discussion. Viral matrix proteins exert their fundamental role in assembly and budding through their interaction with cellular membranes. We have previously characterised the *in vitro* binding properties of three soluble forms of the Ebola virus matrix protein VP40 which showed that (i) the N-terminal 31 residues were dispensable for membrane association; (ii) the C-terminal residues 213 to 326 were absolutely necessary for membrane targeting; (iii) the removal of the C-terminal domain led to hexamerisation of VP40(31–212) (*7*); and (iv) the same hexamerisation pattern can be induced by urea treatment, deletion of seven C-terminal residues, and liposome binding *in vitro* (*12*). The structure of VP40 is composed of two domains that are only weakly associated with each other and we have proposed that a movement of the C-terminal domain induces hexamerisation of VP40 upon membrane association (*11, 12*). Here we show that all three VP40 forms show the same membrane binding properties *in vivo* as observed *in vitro* (*7*), whereas membrane association absolutely requires the C-terminal domain. Interestingly, only a small percentage of VP40, VP40(1–326) as well as VP40(31–326), is asso-

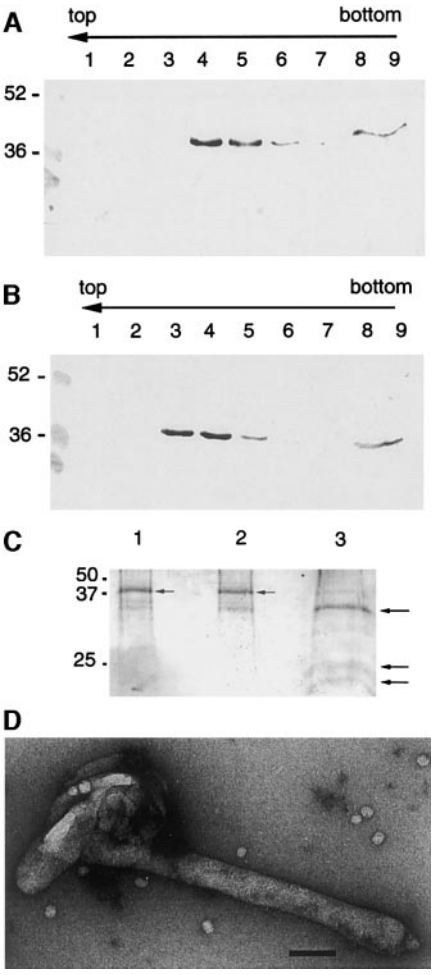

FIG. 4. Sucrose gradient floatation analysis of VP40 released into the cell culture medium; (A) VP40(1–326) and (B) VP40(31–326). Fractions 8 and 9 are part of the bottom fractions which were adjusted to 50% sucrose while fractions 3 to 6 show that most of the released VP40 floats up in the gradient. Fractions from the sucrose gradient were precipitated with TCA and separated on 12% SDS–PAGE. (C) Trypsin digestion of VP40(1–326) found to be associated with lipid vesicles (fraction 4 corresponding to lane 4; Fig. 4A); lane 1, no trypsin; lane 2, 50 ng trypsin; lane 3, solubilisation of vesicles with 1% Triton X-100 and 50 ng trypsin. Full-length VP40 (lanes 1 and 3) and proteolytic products (lane 3) are indicated by arrows. VP40 samples were separated on 15% SDS–PAGE and specific bands were detected by Western blot analysis. Molecular weight markers are indicated. (D) Detection of filovirus-like particles by negative staining electron microscopy. The black bar represents 100 nm. The diameter of the particle is approximately 80 nm and the length of the filamentous structure shown is approximately 1000 nm.

ciated with the plasma membrane in mammalian cells. In addition, our data suggest that VP40, when associated with the plasma membrane, is released into the cell culture supernatant. Sucrose floatation experiments with the cell culture supernatant insinuate that VP40 is associated with lipid vesicles. The protection from trypsin digestion further suggests that VP40 is inside the vesicles. Negative staining electron microscopy provides additional evidence that vesicles, which bud off the plasma membrane, resemble viruslike structures. However, we only detect viruslike particles at a very low efficiency, which probably underlines an important role of other viral proteins in particle formation (*17–20, 22*). Filovirus show a uniform diameter of approximately 80 nm with some variation in length (*23*). These measurements are in agreement with the sizes of the observed filamentous particles released from 293T cells expressing full-length VP40(1–326) or VP40(31–326) (data not shown). Overall, our experiments show that VP40 is able to assemble into particles, most likely at the plasma membrane, which can bud off the membrane. The resulting particles are probably internally lined with VP40, in a process that can be achieved in the absence of any other viral protein.

A similar release of vesicles containing matrix protein has been reported for VSV, another member of the Mononegavirales (*13–15, 24*). VSV M also contains a putative WW domain binding motif (PY motif), which has been suggested to bind to cellular factor(s) which enhance the function of M in assembly and particle release (*15*). Ebola virus VP40 has a similar motif at its N-terminus (*15*) and a recent paper by Harty *et al.* (*16*) shows that the PY motif is important for budding and confers VP40's interaction with Rsp5, a ubiquitin ligase known to function in endocytosis in yeast and in mammalian cells (Nedd4, mammalian homolog of Rsp5). Our finding that the deletion of the complete PY motif sequence [VP40(31–326)] still supports budding albeit to a fivefold decreased efficiency is in agreement with the mutagenesis data of the PY motif which abolished the binding to the ubiquitin ligase and reduced the release of vesicles fourfold (*16*). Interestingly, ubiquitin has also been recently implicated to play an important role in the retroviral budding machinery (*25, 26*) indicating a common mechanism for particle release for retroviruses, filoviruses, and rhabdoviruses. In addition, we provide evidence that the deletion of the PY motif-containing sequence does not affect membrane association of VP40 implied by the same percentage of VP40 found to be associated with the plasma membrane *in vivo* for full-length VP40 as well as for VP40(31–326). These findings are consistent with the data obtained *in vitro* with the liposome binding assays (*7*).

Although we attempted to determine the oligomeric state of VP40 present in the vesicles released from cells, chemical cross-linking experiments generally resulted in high molecular weight bands whose interpretation was not conclusive (data not shown) and could not be clearly related to the hexamers observed *in vitro* (*12*). However, the formation of particles driven by the matrix protein indirectly infers the assembly of higher molecular weight structures by VP40 which eventually provide the architecture for particle release. The release of viruslike particles containing VP40 provides evidence that VP40 is able to "self-assemble" on its own into a higher order structure on membranes, a feature which seems to be a

prerequisite for membrane-containing particle formation. The efficiency of such a process is dependent on the interaction with cellular protein(s) (*16*) and the presence of other viral proteins will most likely enhance the assembly and budding efficiency. Nevertheless, our report and a recent paper by Harty *et al.* (*16*) show that VP40 contains the minimal information necessary to induce release of VP40-containing viruslike particles from mammalian cells.

Materials and Methods. Expression constructs. cDNAs corresponding to full-length VP40, VP40 residues 31 to 326 [VP40(31–326)], and residues 31 to 212 [VP40(31–212)] were cloned into the mammalian expression vector pcDNA 3.1 (Invitrogen) [pVP40(1–326); pVP40(31–326); pVP40(31–212)] and the cDNA corresponding to full-length ADAM12-L (*21*) was cloned into the pSectagB vector (Invitrogen) [pADAM12-L] using standard PCR methods. The correctness of the sequence of each construct was verified by DNA sequencing. The ADAM12-L construct contains a C-terminal myc-epitope.

Cell Line and Transfection. The 293T cells were grown in DMEM medium supplemented with Glutamax I and 4500 mg/ml glucose, 50 unit/ml penicillin, 50 μg/ml streptomycin, and 10% fetal bovine serum (Life Technologies, Inc.) at 37°C and 5% CO_2. 293T cells were grown to 50% confluence and then transfected with 1 μg of plasmid DNA mixed with 5 μl of Lipofectine (Life Technologies, Inc.). Cells and supernatants were collected 3 days posttransfection for further analysis. Whole-cell lysates (2×10^5 cells per lane) and supernatants (corresponding to 2×10^5 cells) were analyzed by Western blot using a VP40 specific antiserum as primary antibody and a secondary anti-rabbit IgG serum conjugated to alkaline phosphatase (Promega). The relative amount of total expressed VP40 (set to be 100%) was compared to the amount released by scanning the intensity of the bands derived from the same amounts of total cells analysed.

Immunofluorescence. Cells were grown on cover glasses and were analyzed by indirect immunofluorescence 3 days posttransfection. Cells were washed 3 times with cold PBS on ice containing 1 mM $MgCl_2$ and 0.1 mM $CaCl_2$ and subsequently permeabilised and fixed with a solution containing ice-cold methanol (80%) and acetone (20%) for 20 min at −20°C. Cells were then blocked with PBS containing 1% BSA for 30 min before being incubated with the primary antibody, a rabbit anti-VP40 serum, or an anti-myc monoclonal antibody (Invitrogen) for 1 h at room temperature. Cells were washed 3 times with cold PBS containing 1 mM $MgCl_2$ and 0.1 mM $CaCl_2$ before the secondary antibody conjugated with fluorescein-isothiocyanate, an anti-rabbit IgG (VP40), or anti-mouse IgG (ADAM-12L) (Life Technologies, Inc.) was added. Cover glasses were mounted in fluoromount-G (Southern Biotechnology Associates, Inc.) and fluorescence staining was visualised using an Axioskop fluorescence microscope (Zeiss).

Membrane Floatation Experiments. Cell culture supernatants of transfected cells were made 50% sucrose (w/v) in a total volume of 5 ml. This was successively overlaid with 2 ml of 40% sucrose (w/v), 2 ml of 35% sucrose (w/v), 2 ml of 20% sucrose (w/v), and 1 ml of 10% sucrose (w/v); all sucrose solutions were prepared in PBS. Gradients were centrifuged using a SW41 rotor at 40,000 rpm for 15 h at 12°C. Seven fractions of 1 ml and two 2.5-ml fractions from the bottom were collected from the gradients and 500 μl of each fraction was precipitated with 3.5% TCA for Western blot analysis. Pellets of each sample were separated on a 12% SDS–PAGE and blotted onto nitrocellulose membranes. VP40 specific bands were visualised by Western blot analysis as described.

Trypsin Digestion. Fifty microliters of fraction 4 from the sucrose gradient containing VP40(1–326) vesicles (Fig. 4A) were incubated with 50 ng trypsin for 1 h at 37°C in PBS buffer or in PBS buffer containing 1% Triton X-100 to solubilise VP40 contained in lipid vesicles. Samples were separated on a 15% SDS–PAGE and VP40 specific bands were detected by Western blot analysis using the amplified Opti-4CN detection kit (Bio-Rad).

Plasma Membrane Preparation. Plasma membranes (PM) were isolated using an isoosmotic homogenisation medium (adapted from Ref. *27*). Seventy-two hours posttransfection the cells were washed and detached in PBS on ice. Cells were pelleted and then resuspended in homogenisation buffer (HB) consisting of 0.25 M sucrose, 10 mM Tris pH 7.4, and 1 mM $MgCl_2$. A mixture of protease inhibitors (Boehringer Mannheim) was also added to the buffer. The cells were homogenised in a Dounce homogeniser and nuclei were harvested by centrifugation at 280 *g* for 10 min. The organelles and plasma membranes were then pelleted at 1500 *g* for 10 min. This pellet was resuspended in HB before mixing it with 2 vol of 2 M sucrose in 10 mM Tris pH 7.4 and 1 mM $MgCl_2$. This mixture was then overlaid with HB and the membranes were purified by ultracentrifugation in a SW41 rotor at 24,000 rpm for 1 h at 4°C. The fraction corresponding to the plasma membranes floated up to the interface. This fraction was collected and diluted 10 times in HB before harvesting the membranes by centrifugation at 3000 *g* for 10 min. The membranes were then resuspended in SDS–sample buffer for Western blot analysis. Total VP40 protein derived from 2×10^5 cells (100%) and protein floating with the membrane fraction corresponding to 2×10^5 cells were then separated on 15% SDS–PAGE and their relative quantity was determined by scanning the intensity of the bands.

Electron Microscopy. Protein samples in PBS buffer were applied to the clean side of carbon on mica (car-

bon/mica interface) and negatively stained with methylamine vanadate, $CH_3NH_2VO_3$ ("NanoVan," Nanoprobes, Inc., Stony Brook, NY) (pH 8.0). Micrographs were taken under low-dose conditions with a Jeol 1200 EX II microscope at 100 kV and a nominal magnification of 40,000×.

ACKNOWLEDGMENTS

We thank Drs. V. Volchkov and O. Dolnik (Marburg) for the VP40 antiserum and Dr. U. Wewer (Copenhagen) for providing the ADAM12 cDNA.

REFERENCES

1. Feldmann, H., and Klenk, H.-D. (1996). Marburg and Ebola viruses. *Adv. Virus Res*. **47,** 1–52.
2. Zaki, S. R., and Peters, C. J. (1997). Viral hemorrhagic fevers. *In* "Diagnostic Pathology of Infectious Diseases" (Connor, D. H., Schwartz, D. A., Manz, H. J., and Lack, E. E., Eds.), pp. 347–364. Appleton and Lange, Stamford, CT.
3. Schnittler, H. J., Mahner, F., Drenckhahn, D., Klenk, H.-D., and Feldmann, H. (1993). Replication of Marburg virus in human endothelial cells. A possible mechanism for the development of viral hemorrhagic disease. *J. Clin. Invest*. **91,** 1301–1309.
4. Geisbert, T. W., and Jahrling, P. B. (1995). Differentiation of filoviruses by electron microscopy. *Virus Res*. **39,** 129–150.
5. Feldmann, H., Bugany, H., Mahner, F., Klenk, H.-D., Drenckhahn, D., and Schnittler, H. J. (1996). Filovirus induced endothelial leakage triggered by infected monocytes/macrophages. *J. Virol*. **70,** 2208–2214.
6. Garoff, H., Hewson, R., and Opstelten, D.-J. E. (1998). Virus maturation by budding. *Microbiol. Mol. Biol. Rev.* **62,** 1171–1190.
7. Ruigrok, R. W. H., Schoehn, G., Dessen, A., Forest, E., Volchkov, V., Dolnik, O., Klenk, H.-D., and Weissenhorn, W. (2000). Structural characterization and membrane binding properties of the matrix protein VP40 of Ebola. *J. Mol. Biol.* **300,** 103–112.
8. Zakowski, J. J., Petri, W. A., and Wagner, R. R. (1981). Role of matrix protein in assembling the membrane of vesicular stomatitis virus: Reconstitution of matrix protein with negatively charged phospholipid vesicles. *Biochemistry* **20,** 3902–3907.
9. Ruigrok, R. W. H., Barge, A., Durrer, P., Brunner, J., Ma, K., and Whittaker, G. R. (2000). Membrane interaction of influenza virus M1 protein. *Virology* **267,** 289–298.
10. Conte, M. R., and Matthews, S. (1999). Retroviral matrix proteins: S structural perspective. *Virology* **246,** 191–198.
11. Dessen, A., Volchkov, V., Dolnik, O., Klenk, H.-D., and Weissenhorn, W. (2000). Crystal structure of the matrix protein VP40 from Ebola virus. *EMBO J*. **19,** 4228–4236.
12. Scianimanico, S., Schoehn, G., Timmins, J., Ruigrok, R. W. H., Klenk, H. D., and Weissenhorn, W. (2000). Membrane association induces a conformational change in the Ebola virus matrix protein. *EMBO J*. **19,** 6732–6741.
13. Justice, P. A., Sun, W., Li, Y., Ye, Z., Grigera, P. R., and Wagner, R. R. (1995). Membrane vesiculation function and exocytosis of wild-type and mutant matrix proteins of vesicular stomatitis virus. *J. Virol.* **69,** 3156–3160.
14. Sakaguchi, T., Uchiyama, T., Fujii, Y., Kiyotani, K., Kato, A., Nagai, Y., Kawai, A., and Yoshida, T. (1999). Double-layered membrane vesicles released from mammalian cells infected with Sendai virus expressing the matrix protein of vesicular stomatitis virus. *Virology* **263,** 230–243.
15. Harty, R. N., Paragas, J., Sudol, M., and Palese, P. (1999). A proline-rich motif within the matrix protein of vesicular stomatitis virus and rabies virus interacts with WW domains of cellular proteins: Implications for viral budding. *J. Virol*. **73,** 2921–2929.
16. Harty, R. N., Brown, M. E., Wang, G., Huibregtse, J., and Hayes, F. P. (2000). A PPxY motif within the VP40 protein of Ebola virus interacts physically and functionally with a ubiquitin ligase: Implications for filovirus budding. *Proc. Natl. Acad. Sci. USA* **97,** 13871–13876.
17. Metsikkö, K., and Simons, K. (1986). The budding mechanism of spikeless vesicular stomatitis virus particles. *EMBO J*. **5,** 1913–1920.
18. Sanderson, C. M., Wu, H. H., and Nayak, D. P. (1994). Sendai virus M protein binds independently to either the F or the HN glycoprotein in vivo. *J. Virol*. **68,** 69–76.
19. Schmitt, A. P., He, B., and Lamb, R. A. (1999). Involvement of the cytoplasmic domain of the hemagglutinin-neuraminidase protein in assembly of the paramyxovirus simian virus 5. *J. Virol*. **73,** 8703–8712.
20. Jin, H., Leser, G. P., Zhang, J., and Lamb, R. A. (1997). Influenza virus hemagglutinin and neuraminidase cytoplasmic tails control particle shape. *EMBO J*. **16,** 1236–1247.
21. Gilpin, B. J., Loechel, F., Mattei, M.-G., Engval, E., Albrechtsen, R., and Wever, U. (1998). A novel, secreted form of human ADAM12 (meltrin α) provokes myogenesis *in vivo*. *J. Biol. Chem.* **273,** 157–166.
22. Schnell, M. J., Buonocore, L, Boritz, E., Ghosh, H. P., Chernish, R., and Rose, J. K. (1998). Requirement for a non-specific glycoprotein cytoplasmic domain sequence to drive efficient budding of vesicular stomatitis virus. *EMBO J*. **10,** 1289–1296.
23. Ellis, D. S., (1987). The filoviridae. *In* "Animal Virus Structure" (M. V. Nermut and A. C. Steven, Eds.), pp. 313–321. Elsevier Science Publishers B. V., Amsterdam.
24. Li, Y., Luo. L., Schubert, M., Wagner, R. R., and Kang, C. Y. (1993). Viral liposomes released from insect cells infected with recombinant baculovirus expressing the matrix protein of vesicular stomatitis virus. *J. Virol*. **67,** 4415–4420.
25. Patnaik, A., Chau, V., and Wills, J. W. (2000). Ubiquitin is part of the retrovirus budding machinery. *Proc. Natl. Acad. Sci. USA* **97,** 13069–13074.
26. Strack, B., Calistri, A., Accola, M. A., Palu, G., and Gottlinger, H. G. (2000). A role for ubiquitin ligase recruitment in retrovirus release. *Proc. Natl. Acad. Sci. USA* **97,** 13063–13068.
27. Hubbard, A. L., Wall, D. A., and Ma, A. (1983). Isolation of rat hepatocyte plasma membranes. I. Presence of the three major domains. *J. Cell Biol.* **96,** 217–229.